Available online at www.sciencedirect.com
ScienceDirect
Journal of Photochemistry and Photobiology A: Chemistry 195 (2008) 151–155
Journal of Photochemistry and Photobiology A:Chemistry
www.elsevier.com/locate/jphotochem

Plus green emission of ZnO nanorods induced by Ce^{3+} doping and concentration

Chao Cheng [a,b], Zhong-Jie Jiang [a], Chun-Yan Liu [a,*]

[a] *Laboratory of Organic Optoelectronic Functional Materials and Molecular Engineering, Technical Institute of Physics and Chemistry, Chinese Academy of Sciences, Beijing 100080, China*
[b] *Graduate School of the Chinese Academy of Sciences, Beijing 100806, China*

Received 31 May 2007; accepted 27 September 2007
Available online 2 October 2007

Abstract

ZnO nanorods and ZnO nanorods doped with Ce^{3+} have been synthesized by a solvothermal method. The properties of as-synthesized nanorods were investigated by TEM, X-ray diffraction and photoluminescence spectroscopy. The results showed that Ce^{3+} doping and increasing concentration could induce the enhancement of photoluminescence.

Keywords: Zinc oxide; Solvothermal; Cerium doping; Green emission; Concentration

1. Introduction

In the recent years, ZnO has attracted much attention of researchers due to its special properties and a potential application. ZnO is a typical semiconductor with a wide band gap of 3.37 eV and a large exciton binding energy of 60 meV at room temperature [1], which provides it a wide application field including optoelectronic devices [2], field-emission transistors [3], light-emitting diodes [4], solar cells [5], nanoresonators [6], and gas sensors [7]. ZnO with different shapes has been synthesized, including nanorods [8], nanowires [9], core–shell nanotubes [10], nanobelts [11], nanoribbons [12], nanotetrapods [13], nanowire-formed microtubes [14], comb-like nano-structures [15] and so on. And one-dimensional single crystalline semiconductors have little surface disorder and less deficiency, which will decrease the contribution of the surface-related nonradiative recombination and are predicted high photoluminescence (PL) efficiency.

The introduction of impurities can modulate the structure of semiconductors and cause dramatic change of photoelectric and optical properties [16]. In the case of transition metals or rare-earth elements, the radiative efficiency of the impurity-induced emission increases significantly. It is possible to get more interesting PL properties when transition metals are introduced into the lattice of semiconductor nanorods and nanowires.

Thus, doping impurities into one-dimensional ZnO nanostructure to improve the band-gap structure and PL properties is worthy to be explored. However, although much work has been done to investigate the optical properties of transition metal or rare-earth metal doped semiconductor particles, the study on the optical properties of rare-earth ions doped one-dimensional ZnO nano-structure is seldom, probably due to rare-earth ions limited solubility and larger radius compared with Zn^{2+}.

In this work, we synthesized Ce^{3+} doped ZnO nanorods using a simple solvothermal method and investigated the PL properties of the sample. The results indicated that the rare-earth ions could be partly doped into ZnO lattice and greatly change the PL properties of ZnO nanorods. The changes in emission intensity with Ce^{3+} doping were attributed to the lattice defects increase caused by Ce^{3+} doping into ZnO lattice.

Besides doping, there might be other factors that could effect on PL intensities of ZnO nanorods. Here, we changed our sample concentration during PL testing and found PL intensities increased with increasing the concentration.

* Corresponding author. Tel.: +86 10 82543573; fax: +86 10 62554670.
E-mail address: cyliu@mail.ipc.ac.cn (C.-Y. Liu).

1010-6030/$ – see front matter © 2007 Elsevier B.V. All rights reserved.
doi:10.1016/j.jphotochem.2007.09.017

2. Experimental

2.1. Materials

Zinc acetate dihydrate [$Zn(Ac)_2{\cdot}2H_2O$, >99%], sodium hydroxide (NaOH, >99%), anhydrous ethanol and cerium nitrate hexahydrate [$Ce(NO_3)_3{\cdot}6H_2O$, >99%] are all obtained from Beijing Chemical Reagents Co. and used without further purification.

2.2. Synthesis

The synthesis of ZnO nanorods was performed using a solvothermal method described by Cheng and Samulski [21] and Pacholski et al. [22]. Typically, 40 mL 0.25 M NaOH solution in ethanol was added to 20 mL 0.05 M $Zn(Ac)_2{\cdot}2H_2O$ ethanol solution, and the mixture was stirred for about 30 m. Then, it was transferred to a Telfon-lined stainless steel autoclave and heated at 150 °C for 24 h. The system was allowed to cool to room temperature and a final product was collected, washed with distilled water and ethanol for several times, separated by a centrifuge, and then dried in the air.

Ce^{3+} doped ZnO nanorods was synthesized by a similar approach as described above, except for the addition of $Ce(NO_3)_3{\cdot}6H_2O$ into $Zn(Ac)_2{\cdot}2H_2O$ solution before the addition of NaOH solution. The quantities of $Ce(NO_3)_3{\cdot}6H_2O$ added was varied to get different doping concentration of Ce^{3+} in ZnO nanorods. And thermal annealing to as-synthesized samples at 500 °C for 3 hours was taken to discuss the origin of the deep-level emission.

2.3. Characterization

Transmission electron microscopy (TEM) images of samples and selected area electron diffraction (SAED) were obtained with a JEOL JEM-CX200 microscope operating at 160 kV. The samples were prepared by ultrasonically dispersing the products in ethanol, and dropped onto a Formvar coated copper grid (200 mesh; placed onto filter paper to remove excess solvent). The solvent evaporated and dried in the air at room temperature.

X-ray powder diffraction (XRD) patterns were measured using Rigaku DMAX-RB X-ray diffractometer with the Cu Kα radiation (λ = 1.5406 Å), operating at 40 kV. The samples for XRD were repeatedly rinsed and dried at 80 °C for more than 10 h. And then it was put onto glass substrates for measurements.

The spectra of the products were recorded on a Hitachi F-4500 fluorescence spectrometer with a lamp source of 150 W Xenon. The samples were well dispersed in ethanol by ultrasonication and prepared with different concentration, from an original concentration of 0.1 mg/mL to a diluted concentration of 0.01 mg/mL. Measurements were performed using a quartz cell with a path length of 10 mm. The intensity of emitted light was detected at a right angle to the incident light.

3. Results and discussion

As shown in Fig. 1, the average diameter of ZnO nanorods was around 40 nm and the aspect ration was larger than 10 (Fig. 1a). The introduction of Ce^{3+} ions induced the changes of the size and morphology of final products. It is extremely evident that the width of the ZnO rod doped with Ce^{3+} ions increased and the aspect ratio decreased (Fig. 1b and c). The SAED patterns (the insert in Fig. 1a–c) indicated that the nanorods were single-crystalline ZnO with a wurtzite structure. In addition, some small particles were also observed in Fig. 1b and c. The lattice constants calculated from the ED rings in Fig. 1d showed that the small particles (in Fig. 1b and c) were not ZnO but Ce impurity,

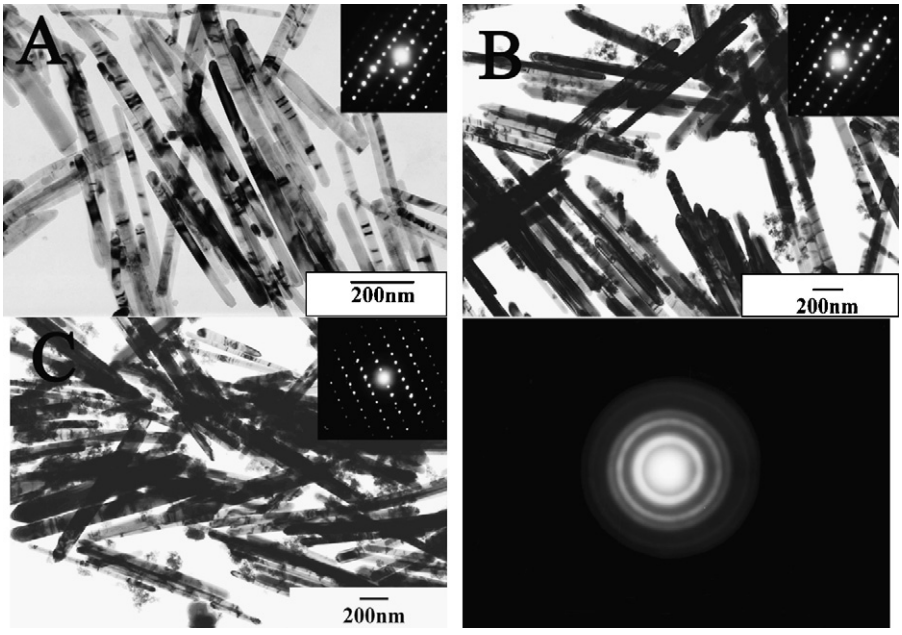

Fig. 1. Typical TEM images of ZnO nanorods doped with Ce^{3+} ions. (a) Undoped; (b and c) doped with 1.0% and 3.0% Ce^{3+}, respectively. (d) ED pattern of small particles in (b and c). The inset was SAED patterns of corresponding ZnO nanorods.

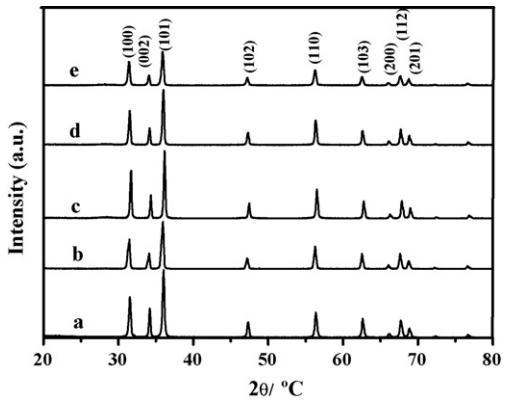

Fig. 2. Power XRD patterns of as-synthesized ZnO doped with Ce^{3+} ions, (a) undoped; (b–e) doped with the initial Ce^{3+} concentration of 0.5%, 1.0%, 2.0% and 3.0%, respectively.

indicated that Ce^{3+} ions could only partly dope into the ZnO rods and others were excluded out of ZnO lattices during the solvothermal process.

Fig. 2 showed the powder XRD patterns of as-synthesized ZnO. Sharp diffraction peaks corresponding to a hexagonal wurtzite structure of ZnO particles were observed, indicating the ZnO rods prepared by the present method are highly crystallized. The lattice constants ($a = 3.27$ Å and $c = 5.24$ Å) of the undoped samples calculated from the XRD pattern are closed to the standard values of the reported bulk ZnO (JCPDS file, No. 367-1451, $a = 3.249$ Å, $c = 5.2066$ Å). While the lattice parameter c increased from 5.239 Å of the sample undoped to 5.251 Å of the sample doped with the lowest concentration of 0.5% Ce^{3+}(calculated from the (0 0 2) peak of each sample). The increase of the lattice parameters revealed that Ce^{3+} ions have been incorporated into the ZnO lattice and substituted the Zn^{2+} ion sites, since the ionic radius of Ce^{3+} (1.03 Å) is much bigger than that of Zn^{2+} (0.74 Å). The possible reason that Ce^{3+} ions could be doped into ZnO rods was due to the high pressure of the hydrothermal process, which pressed the Ce^{3+} ion into the lattice of ZnO.

PL spectra of ZnO and Ce^{3+}doped ZnO at room temperature were showed in Fig. 3a. It can be seen that there were two apparent emission peaks in the spectra, in good agreement with previous reports [17]. One was at about 381 nm, corresponding to the near band edge emission. The other was the green emission band centered at about 500 nm, which is commonly referred to as the recombination of electrons in single occupied oxygen vacancies with photogenerated holes [18]. As Fig. 3a shown, the doping of Ce^{3+} into ZnO nanorods could increase the green emission intensity obviously. When the doping concentration reached 1%, the green emission intensity got a maximum in our experimental condition.

Fig. 3b was PL excitation spectra of the samples. Similar to the emission spectra, ZnO nanorods doped with 1% Ce^{3+} exhibited a maximum intensity. The peaks of the excitation spectra appeared at about 366 nm, corresponding to the energy gap of ZnO.

Previous work [17] has showed that the increase of the width of ZnO nanorods and the decrease of aspect ratio did not influence the PL properties of ZnO nanorods so much. Therefore, the changes of the PL intensities are mainly caused by doping of Ce^{3+}.

Generally green emission was attributed to deep trapped energy level caused by defects in ZnO lattices, but which type

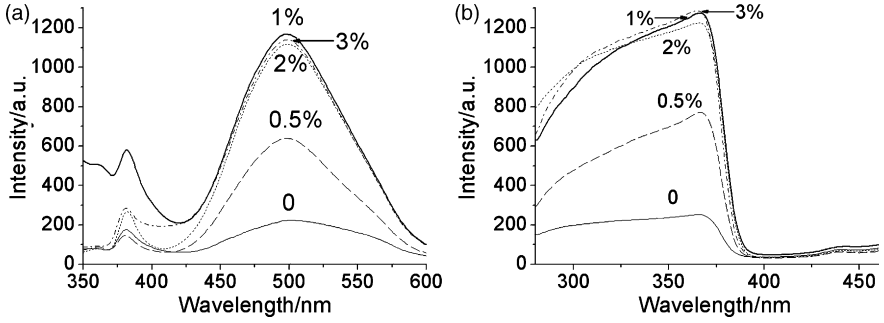

Fig. 3. PL and PL excitation spectra of ZnO nanorods doped Ce^{3+} with ions excited by 325 nm (a) emission spectra excited by 325 nm (b) excitation spectra detected at 500 nm.

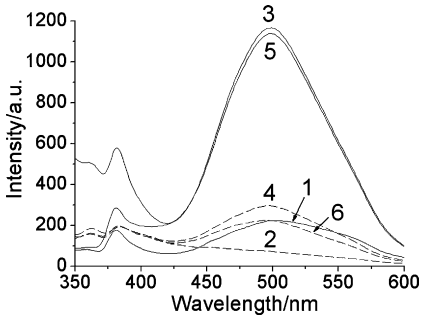

Fig. 4. PL spectra of ZnO nanorods before and after thermal annealing at 500 °C, excited by 325 nm. (1) (2) undoped, before and after annealing; (3) (4) 1% doping, before and after annealing; (5) (6) 3% doping, before and after annealing.

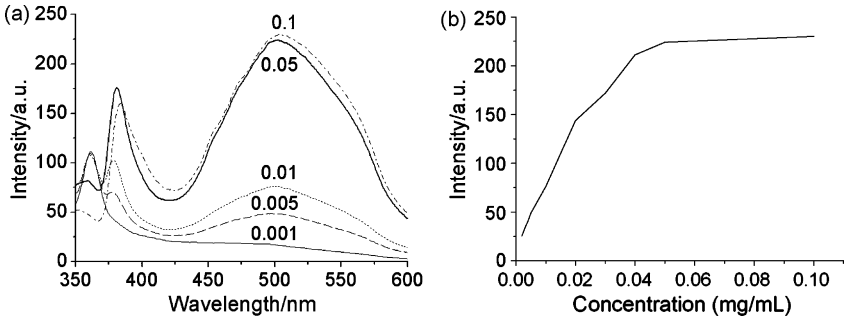

Fig. 5. PL spectra and maximum green emission intensities of ZnO nanorods undoped prepared at different concentration.

of defects caused the green emission was not clear yet, now. Commonly, available explanation was recombination of photoelectrons and singly occupied oxygen vacancies $V_O^{\bullet}$ [18]. Besides, other defects such as zinc interstitial Zn_i [19], oxide antisite defect O_{Zn} [20] were also introduced as possible reasons. In our work, however, the enhancement of the green emission intensities might be attributed to lattice defects increase caused by Ce^{3+} doping into ZnO lattice. Thermal annealing could decrease deep-level defects, and result in a reduction of deep-level emission. Thus, the samples undoped and doped with 1%, 3% Ce^{3+} were heated at 500 °C for 3 hours. Fig. 4 showed the PL spectra change of samples before and after thermal annealing. For all the three samples, obvious reduction of green emission was found, which proved the green emission came from deep-level lattice defects.

The PL spectra of the naked ZnO in ethanol with different concentrations were shown in Fig. 5. There were three evident peaks in most cases. The UV peak and green peak appeared at about 380 nm and 500 nm, as mentioned above. An extra peak appeared at about 360 nm and the intensity became higher at low concentration. From the blank PL measurement of ethanol, it could be confirmed that the 360 nm peak came from ethanol. At a low concentration of ZnO, the UV peaks at 380 nm could not be observed, perhaps the weaken emissions were covered up by the 360 nm peaks of ethanol.

As shown in Fig. 5a, both the UV emission intensity and green emission intensity increased with the concentration of the pure ZnO. The green emission intensity as a function of the concentration showed in Fig. 5b. It can be found that there was a fine linear relation between the intensity and sample concentration at the concentration lower than 0.02 mg/mL. At a higher concentration, the increasing speed of the intensity reduced. This could be explained by Lambert–Beer's law:

$$I_t = I_0 e^{-\varepsilon c l} \tag{1}$$

where ε and c represent extinction coefficient and concentration of the sample solution, respectively, and l is the path length of the light in the solution.

As shown in Fig. 6 , considering a thin liquid layer dx with a distance x to the surface of the solution, using dI and dF to represent light energy absorbed by this thin layer and fluorescence emission intensity, we can get:

$$dF = K\,dI \tag{2}$$

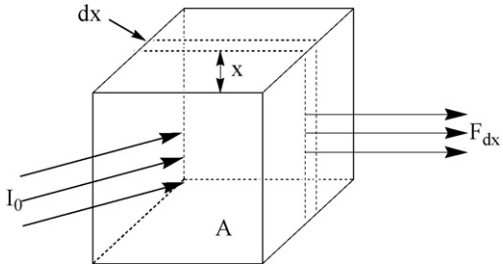

Fig. 6. A sketch map of fluorescence in the solution.

Light intensities before and after entering this thin layer can be calculated as $I_0 e^{-\varepsilon c x}$ and $I_0 e^{-\varepsilon c(x+dx)}$, so:

$$dI = I_0[e^{-\varepsilon c x} - e^{-\varepsilon c(x+dx)}] = I_0 e^{-\varepsilon c x}[1 - e^{-\varepsilon c\,dx}] \tag{3}$$

As $\varepsilon c\,dx$ is a small amount, we can get:

$$dI = I_0 e^{-\varepsilon c x} \varepsilon c\,dx \tag{4}$$

After making the substitution of Eq. (4) into Eq. (2), we can obtain:

$$dF = K I_0 \varepsilon c\, e^{-\varepsilon c x}\,dx \tag{5}$$

Fluorescence intensity of the solution is an integral though the whole light path length l, that is:

$$\begin{aligned} F &= K I_0 \varepsilon c \int_0^l e^{-\varepsilon c x}\,dx = K I_0 (1 - e^{-\varepsilon c l}) \\ &= K I_0 \left[\varepsilon c l - \frac{(\varepsilon c l)^2}{2!} + \frac{(\varepsilon c l)^3}{3!} - \cdots \right] \\ &= K I_0 \varepsilon c l \left[1 - \frac{\varepsilon c l}{2} + \frac{(\varepsilon c l)^2}{6} - \cdots \right] \end{aligned} \tag{6}$$

The experimental values of PL intensities and the concentration of the sample were fitted well, using the Eq. (6), as shown in Fig. 7 . At a low concentration, emission intensities increased with concentration, as light-emitting centers increased at a higher concentration. When the concentration was higher than a certain value, the emission intensity would reduce, because the interaction of light-emitting centers became drastic. The maximum emission intensity appeared at the concentration of about 0.07 mg/mL. Extinction coefficient ε can be calculated using Eq. (6), where $c = 1/\varepsilon l$ is the concentration corresponding to the

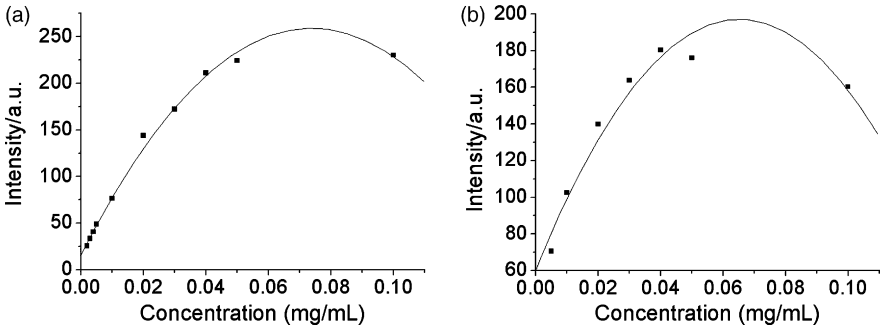

Fig. 7. Peak value of green emission (a) and UV emission intensity (b) vs. the sample concentration and fitting curve based on the Eq. (6).

strongest emission peak. The calculated results show, the emission peak intensity for green and UV emission are 0.0738 and 0.0652 mg/mL respectively. The average value 0.0695 mg/mL is used to calculate ε. In our experiment l equals to 1 cm, so ε is 14.39 L/g·cm.

The same tests were also carried out with the samples doped Ce^{3+}, and similar results were obtained.

4. Conclusions

ZnO nanorods doped with different concentrations of Ce^{3+} ions have been synthesized by a simple solvothermal process. Results showed that the doping of Ce^{3+} ions greatly changed the PL properties of the ZnO nanorods, which could be caused by lattice defects increase due to Ce^{3+} doping into ZnO lattice. Naked samples dispersed in ethanol with different concentrations showed different PL spectra and emission intensities accorded Lambert–Beer's law.

Acknowledgments

The author thanks the support of National Natural Foundation of China (20573126) and Chinese Academy of Sciences.

References

[1] C. Klingshirn, Phys. Stat. Sol. B 71 (1975) 547.
[2] M.H. Huang, S. Mao, H. Feick, Science 292 (2001) 1897.
[3] J. Goldberger, D.J. Sirbuly, M. Law, J. Phys. Chem. B 109 (2005) 9.
[4] C.H. Liu, J.A. Zapien, Y. Yao, Adv. Mater. 15 (2003) 838.
[5] J.B. Baxter, E.S. Aydil, Appl. Phys. Lett. 86 (2005) 0531141.
[6] X.D. Bai, P.X. Gao, Z.L. Wang, Appl. Phys. Lett. 82 (2003) 4806.
[7] Q. Wan, Q.H. Li, Y.J. Chen, Appl. Phys. Lett. 84 (2004) 3654.
[8] Y.J. Tak, K.J. Yong, J. Phys. Chem. B 109 (2005) 19263.
[9] H.B. Huang, S.G. Yang, J.F. Gong, J. Phys. Chem. B 109 (2005) 20746.
[10] X.Y. Kong, Y. Ding, Z.L. Wang, J. Phys. Chem. B 108 (2004) 570.
[11] Z.W. Pan, Z.R. Dai, Z.L. Wang, Science 291 (2001) 1947.
[12] Z. Gui, J. Liu, Z.Z. Wang, J. Phys. Chem. B 109 (2005) 1113.
[13] Z. Chen, Z.W. Shan, M.S. Cao, Nanotechnology 15 (2004) 365.
[14] J.S. Jeong, J.Y. Lee, J.H. Cho, Chem. Mater. 17 (2005) 2752.
[15] H.Q. Yan, R.R. He, J.J. Johnson, J. Am. Chem. Soc. 125 (2003) 4728.
[16] K.J. Kim, Y.R. Park, Appl. Phys. Lett. 78 (2001) 475.
[17] Z.Q. Li, Y.J. Xiong, Y. Xie, Inorg. Chem. 42 (2003) 8105.
[18] K. Vanheusden, W.L. Warren, C.H. Seager, J. Appl. Phys. 79 (1996) 7983.
[19] N.O. Korsunska, L.V. Borkovska, B.M. Bulakh, J. Lumin. 102–103 (2003) 733.
[20] B.X. Lin, Z.X. Fu, Y.B. Jia, Appl. Phys. Lett. 79 (2001) 943.
[21] B. Cheng, E.T. Samulski, Chem. Commun. (2004) 986.
[22] C. Pacholski, A. Kornowski, H. Weller, Angew. Chem. Int. Ed. 41 (2002) 1188.